

1 **The Spillover of Tropospheric Ozone Increases has hidden the Extent of**
2 **Stratospheric Ozone Depletion by Halogens**

3 **Michael J. Prather¹**

4 ¹Department of Earth System Science, University of California, Irvine, CA, USA

5 Corresponding author: Michael Prather (mprather@uci.edu)

6 **Key Points:**

7 • Our world has seen damaging levels of ozone depletion over the past several decades,
8 and these will continue into this century

9 • Ozone column changes are a combination of halogen-driven stratospheric decreases
10 counteracted by pollution-driven tropospheric increases

11 • Tropospheric increases spillover into the stratosphere and thus the observed recovery of
12 assumed halogen-driven loss is overestimated

13

14 Abstract

15 Stratospheric ozone depletion from halocarbons is partly countered by pollution-driven increases
16 in tropospheric ozone. While recognizing this, the ozone assessment's evaluation of observations
17 and processes have often split the chapters at the tropopause boundary. Using a chemistry-
18 transport model we find that air-pollution ozone enhancements in the troposphere spill over into
19 the stratosphere at significant rates, i.e., 13%-34% of the excess tropospheric burden appears in
20 the lowermost extra-tropical stratosphere. As we track the anticipated recovery of the observed
21 ozone depletion, we should recognize that two tenths of that recovery may come from the
22 transport of increasing tropospheric ozone into the stratosphere.

23

24 Plain Language Summary

25 The world has made great strides in phasing out the halocarbons that drive ozone loss, such as
26 the chlorofluorocarbons 11 and 12. While living with the well-documented depletion of the
27 ozone layer, we are now watching the slow recovery (increase) of stratospheric ozone over this
28 century after our phaseout of halocarbon production and use. Projecting this recovery date also
29 depends on the impact of other changing greenhouse gases on stratospheric chemistry as well as
30 changes in tropospheric ozone. Both observations and models identify tropospheric ozone as
31 increasing due to air-quality pollution in the lower atmosphere. Here, using a global chemistry-
32 transport model, we find that this ozone increase carries over into the stratosphere at rates
33 affecting the recovery expected from the decay of atmospheric halocarbons. This process is
34 inherently included in our chemistry-climate models but is not diagnosed as such. The ozone
35 assessments need consider that what happens in the troposphere does not stay in the troposphere,
36 complicating our interpretation of ozone changes over this century.

37 0 Prologue

38 The *Climatic Impact Assessment Program* (CIAP, 1974) in the early 1970s completed an
39 integrated U.S. assessment of the ozone (O_3) layer as being under future threat from a proposed
40 fleet of high-flying Concorde-like supersonic transport aircraft (SSTs). The threat of depletion
41 of the ozone layer was based on the catalytic ability of oxides of nitrogen (NOx) emitted from
42 the engines to destroy stratospheric ozone (Johnston, 1971; McElroy et al., 1974). The
43 hypothetical threat of SSTs was quickly replaced by real ozone depletion caused by
44 chlorofluorocarbons (Molina and Rowland, 1974; Stolarski and Cicerone, 1974; Wofsy and
45 McElroy, 1974). Ozone assessments became international and remained focused on halogen-
46 driven ozone depletion (e.g., WMO, 1981; 1985; 2022). In 1988 the NASA *High Speed*
47 *Research Program* revived the dream of a commercial SST fleet and initiated the *Atmospheric*
48 *Effects of Stratospheric Aircraft* (AES) to re-assess SST impacts based on the maturity of
49 stratospheric science. In the first AES report, a figure appeared (Schmeltekopf, 1992;
50 reproduced here as **Fig. 1**) that predicted increases in lowermost stratospheric O_3 from the
51 aircraft NOx due to "smog reactions" that include methane (CH_4). This result was surprising at
52 first to those focusing on O_3 depletion, and it may be the first assessment to show increased
53 lower stratospheric O_3 production associated with human pollution.

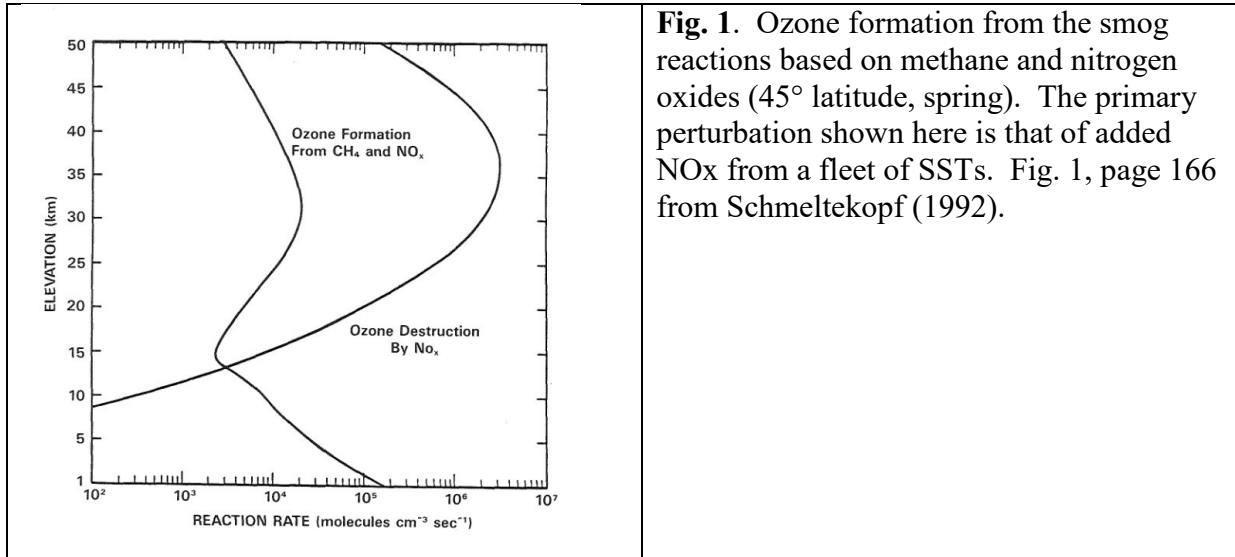


Fig. 1. Ozone formation from the smog reactions based on methane and nitrogen oxides (45° latitude, spring). The primary perturbation shown here is that of added NO_x from a fleet of SSTs. Fig. 1, page 166 from Schmeltekopf (1992).

54

55 1 Introduction

56 The community has continued to study pollution of the lower stratosphere whereby ozone
 57 precursors or ozone-depleting substances are transported from the troposphere into the
 58 stratosphere, thereby altering the chemical production and loss of O₃. Some examples include
 59 the convective overshooting at the tropical tropopause (Oman et al., 2016; Wales et al., 2018),
 60 the South Asian Monsoon (Fu et al., 2006; Randall et al., 2010; Lelieveld et al., 2018; Dubé et
 61 al., 2022), and extensive wildfires (Hirsch and Koren, 2021; Santee et al., 2022; Solomon et al.,
 62 2022), all of which can lead to increases or decreases of stratospheric O₃. What is less studied is
 63 the direct impact of enhanced tropospheric O₃ on the stratosphere. This spillover effect,
 64 whereby tropospheric O₃ pollutes the stratosphere directly rather than through precursors, is not
 65 readily diagnosed because separating the chemistry and transport of O₃ across the tropopause
 66 region is impossible with just O₃ observations and remains a difficult task in most models.

67 In climate forcing, increased tropospheric O₃ dominates stratospheric depletion. Gauss et al.
 68 (2006) in their multi-model assessment recognized that "tropospheric ozone increase since
 69 preindustrial times has moderated lower stratospheric ozone depletion", but they did not have the
 70 scenarios or diagnostics to evaluate it. Other model studies (Shindell et al., 2013; Reader et al.,
 71 2013) derived the amount of tropospheric "pollution" O₃ in the stratosphere but their pollution
 72 scenarios included also the increase in CH₄. Given the very large impact CH₄ has on
 73 stratospheric O₃ (see Fig. 1, and Fig. 14 of Zeng et al., 2022) this obfuscates their results. In the
 74 AerChemMIP study (Collins et al., 2016) a scenario singling out the O₃-precursor emissions
 75 without changing CH₄ provided an opportunity for Zeng et al. (2022) to identify direct O₃
 76 transport, but, even with this scenario, O₃ precursors are emitted directly into the lower
 77 stratosphere (e.g., 18%-44% of aviation NO_x, Gettelman and Baugcum, 1999) or transported
 78 there.

79 In this paper, a set of carefully designed chemistry-transport model (CTM) simulations is
 80 used to assess the impact of direct O₃ influx from the troposphere into the stratosphere. These
 81 simulations follow from the use of direct O₃ emissions to derive the lifetime of tropospheric O₃
 82 (Prather and Zhu, 2024). Given a 20th century tropospheric column O₃ (trpcolO₃) increase of

83 about 9 Dobson Units (DU) (Gauss et al., 2006; Young et al., 2013; Griffiths et al., 2021), this
 84 work identifies a 2-3 DU increase in stratospheric column O₃ (strcolO₃) without including any
 85 stratospheric increase in O₃ precursors such as NO_x and CH₄. Failure to recognize trends of this
 86 level can notably alter the projected year-of-recovery for stratospheric ozone depletion in
 87 response to policy options (see Fig. ES-1 and 3-24 of WMO, 2022) and also the projected net
 88 integrated ozone depletion (Pyle et al., 2022). While this trpcolO₃ spillover is inherently
 89 included in current models, it is likely misdiagnosed in both models and observations as reduced
 90 levels of strcolO₃ depletion and earlier recovery. Modeling is covered in Section 2; analysis of
 91 past and future ozone changes are in Section 3; and a summary discussion is in Section 4.

92 **2 Modeling**

93 **2.1 The UCI chemistry modules**

94 The UC Irvine CTM, like many early CTMs, developed separate chemistry modules for
 95 stratosphere (Linoz: McLinden et al., 2000; Hsu and Prather, 2009; 2010) and troposphere
 96 (ASAD: Wild and Prather, 2000; Wild et al., 2003). The current stratospheric chemistry module
 97 (Linoz version 3) calculates the chemical production and loss of O₃, NO_y (the family of nitrogen
 98 oxides except N₂O), N₂O, and CH₄ as a first-order Taylor expansions about 3D climatological
 99 means (monthly, latitude by pressure) of these species. The expansion also allows for
 100 independent variations in temperature and overhead column O₃. Local stratospheric H₂O is
 101 inferred from CH₄ decay through conservation of H and a tropopause boundary condition of 3.65
 102 ppm (micromol mol⁻¹) H₂O. For the present-day (circa year 2000) simulations shown here the
 103 CTM uses lower tropospheric boundary conditions (LBCs) of 30 ppb (nmol mol⁻¹) for O₃, 0.02
 104 ppb for NO_y, 316 ppb for N₂O, and 1800 ppb for CH₄. Rapid O₃ loss driven by heterogeneous
 105 chemistry on polar stratospheric clouds uses the Cariolle et al. (1990) parameterization, which
 106 produces an excellent simulation of the mean and interannual variability of the Antarctic ozone
 107 hole (e.g., Fig. 8 of Ruiz and Prather, 2022).

108 To calculate the chemical rates and the Taylor expansions, a stratospheric chemistry box
 109 model (Pratmo: e.g., Dubé et al., 2022) is linearized about the climatological mean values of the
 110 independent species scaled to the LBCs for N₂O and CH₄, plus stratospheric climatologies for
 111 the nitrogen (NO_y), chlorine (Cly) and bromine (Bry) families of species. The Pratmo
 112 calculation forces all the individual species in each of the three families to be in 24-hour photo-
 113 stationary state. During a CTM simulation, stratospheric CH₄, N₂O, and NO_y may evolve in
 114 response to changing LBCs, but the Cly and Bry remain fixed per the initial calculation of the
 115 Linoz tables, i.e., 3.24 ppb peak Cly and 16.8 ppt peak Bry for year 2000. The tropospheric
 116 chemistry module ASAD includes about 30 species with a reduced set of hydrocarbon reactions,
 117 but no halogen chemistry. Many ASAD species are set to decay slowly in the stratosphere; but
 118 the NO_y species are reconciled to the Linoz production and loss of NO_y by adjusting NO, NO₂
 119 and HNO₃ to ensure the observed relative influx of these species into the troposphere generated
 120 from the N₂O loss.

121 The choice of which chemistry to apply in each air parcel is triggered by the e90 surface
 122 tracer (Prather et al., 2011) using a threshold of 90 ppb. Thus, a full-chemistry CTM simulation
 123 includes both a standard O₃ tracer that experiences Linoz chemistry when in the stratosphere and
 124 ASAD chemistry when in the troposphere. It also includes a tagged tracer O₃S that experiences
 125 only Linoz chemistry plus the LBC, which is invoked by the Linoz module. A recent example of
 126 the full-chemistry simulations are shown in Prather and Zhu (2024, see their Table 1). Present-

127 day tropospheric O₃ budgets are similar to recent model intercomparison projects (Young et al.,
 128 2018; Griffiths et al., 2021).

129 **2.2 Identifying the Spillover Effect**

130 The work here was triggered by the belated discovery that the O₃ and O₃S tracers in the UCI
 131 CTM differed, not just in the troposphere as expected (where O₃ has ASAD chemistry and O₃S
 132 has only a LBC reset), but also in the lower stratosphere (where both are subject only to the same
 133 Linoz chemistry). To study this effect we set up some diagnostic experiments. First, we
 134 calculate O₃S with two Linoz-only simulations using O₃S LBCs of (a) 10 and (b) 30 ppb.
 135 Finally, we run a full-chemistry simulation (c) with O₃ calculated from the chemical rates in the
 136 troposphere and the O₃S tracer in that run with a 30 ppb LBC. All simulations here are run for
 137 two years using years 2000-2001 meteorological data, with diagnostics taken from the final year
 138 2001. All O₃ diagnostics here are based on sampling all grid cells (320 x 160 x 57) on the 1st of
 139 each month to ensure a clean separation of stratosphere and troposphere based on the e90 tracer
 140 value in each cell. The typical approach using monthly means destroys the tropopause
 141 information, creating a high bias for O₃ (see Prather and Zhu, 2024, who chose 5-day sampling
 142 for better temporal resolution). The global, annual mean, 60°S-60°N profiles of tropospheric O₃
 143 (or O₃S) averaged on model layers are shown in Figure 2a. These profiles include only and all of
 144 tropospheric air. Mean trpcolO₃ values are (a) 8.5 DU, (b) 20.9 DU, and (c) 32.0 DU. The full
 145 chemistry (c) values for trpcolO₃ are our best simulation of the 2000s decade and are consistent
 146 with the observed columns (about 30 DU) and the seasonal cycle (minimum in DJF) found by
 147 Ziemke et al. (2012). The annual mean strcolO₃ for the full chemistry run is 280 DU. As
 148 expected, the O₃S profiles with 30 ppb LBC, either alone (b) or with tropospheric chemistry (c),
 149 are essentially identical and not shown.

150 The profiles in Figure 2b are for stratospheric air only and show the percent difference of O₃
 151 (full) – O₃S (30 ppb) (*blue*) and O₃S (10 ppb) – O₃S (30 ppb) (*red*). The annual mean strcolO₃
 152 difference in these two pairs is +3.8 DU and -1.6 DU, respectively. For both cases the relative
 153 differences in stratospheric O₃ are largest (5-20%) below 16 km and negligible above 22 km.
 154 Absolute differences in the lowermost stratosphere below 19 km for these two cases are nearly
 155 constant at about +30 ppb and -15 ppb, respectively (not shown, but see Fig. 3). Both trace
 156 species O₃ and O₃S experience only Linoz chemical tendencies in the lower stratosphere. These
 157 tendencies drive the O₃ species toward the O₃S profile, the preferred chemical state in the
 158 stratosphere, and thus damp any injection of tropospheric O₃. Any flux of pollution precursors
 159 (e.g., ASAD's NO, CO, H₂O₂) into the stratosphere will be ignored by Linoz. Thus we are
 160 certain that the stratospheric enhancements observed here are due entirely to the transport of
 161 tropospheric O₃ into the stratosphere.

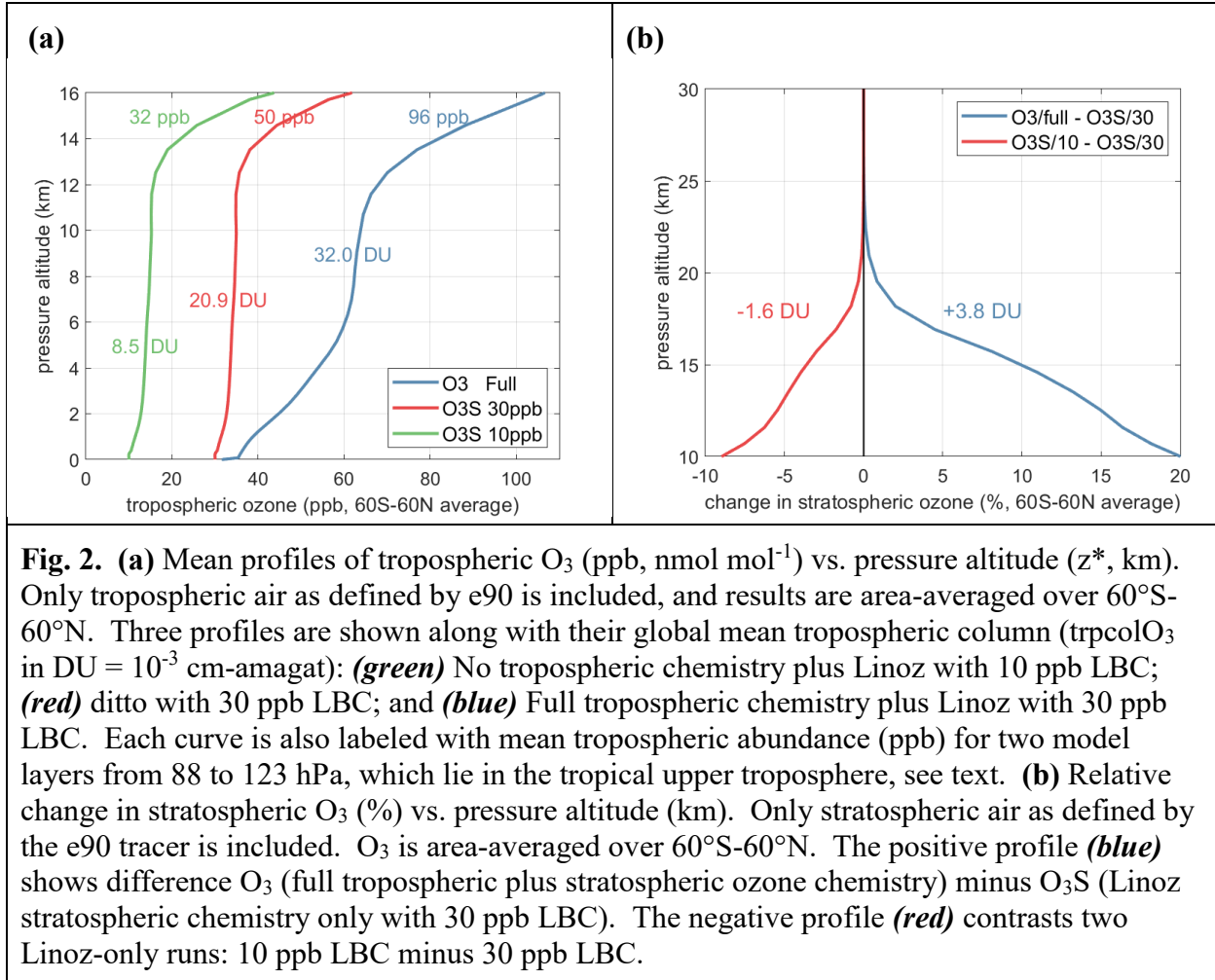
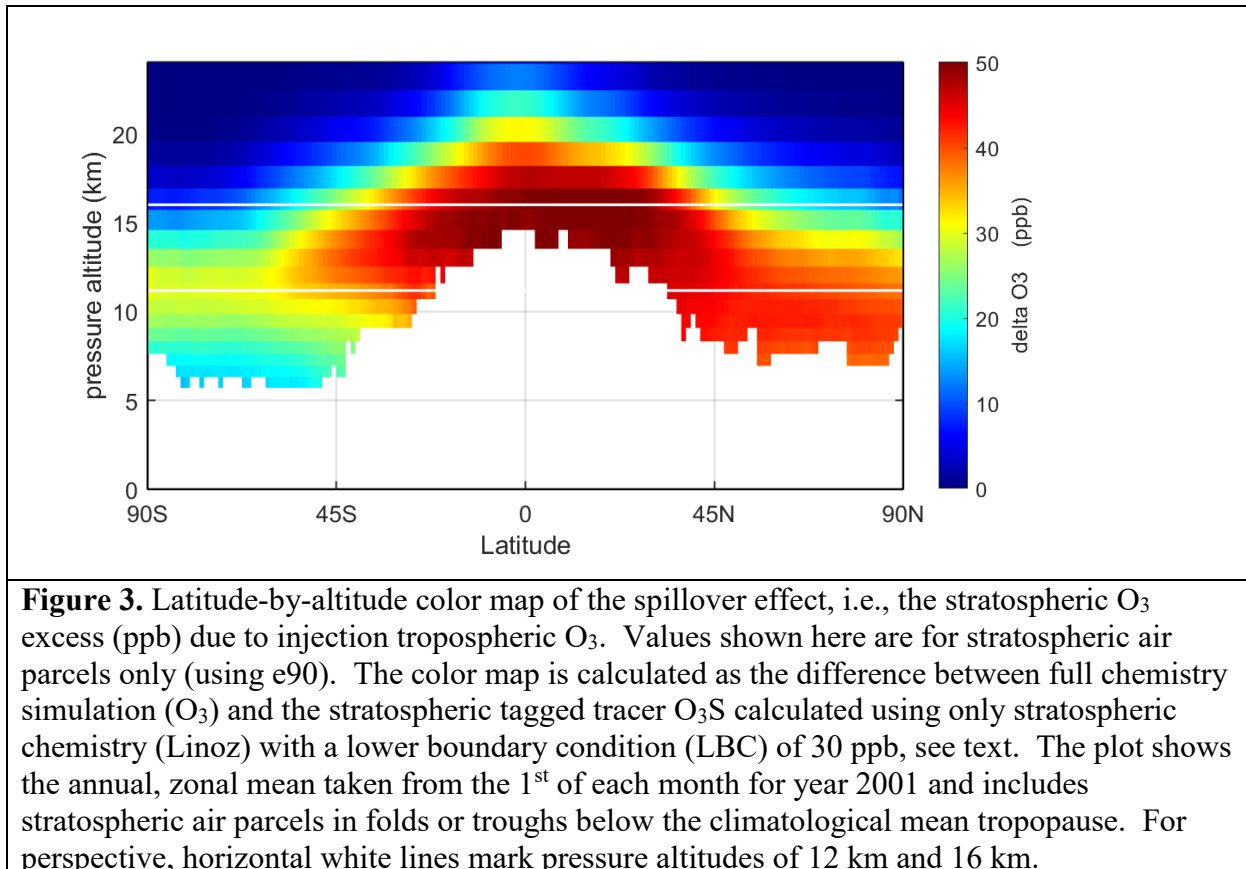


Fig. 2. (a) Mean profiles of tropospheric O_3 (ppb, nmol mol^{-1}) vs. pressure altitude (z^* , km). Only tropospheric air as defined by e90 is included, and results are area-averaged over 60°S - 60°N . Three profiles are shown along with their global mean tropospheric column (trpcol O_3 in DU = 10^{-3} cm-amagat): (**green**) No tropospheric chemistry plus Linoz with 10 ppb LBC; (**red**) ditto with 30 ppb LBC; and (**blue**) Full tropospheric chemistry plus Linoz with 30 ppb LBC. Each curve is also labeled with mean tropospheric abundance (ppb) for two model layers from 88 to 123 hPa, which lie in the tropical upper troposphere, see text. **(b)** Relative change in stratospheric O_3 (%) vs. pressure altitude (km). Only stratospheric air as defined by the e90 tracer is included. O_3 is area-averaged over 60°S - 60°N . The positive profile (**blue**) shows difference O_3 (full tropospheric plus stratospheric ozone chemistry) minus O_3S (Linoz stratospheric chemistry only with 30 ppb LBC). The negative profile (**red**) contrasts two Linoz-only runs: 10 ppb LBC minus 30 ppb LBC.

162 Figure 3 provides a latitude by pressure-altitude color map of the absolute increase in
 163 stratospheric O_3 attributable to excess tropospheric O_3 , calculated as O_3 minus O_3S with a 30 ppb
 164 LBC. We calculate that 99% of the increased mass occurs below 21 km. As in Fig. 2,
 165 stratospheric values from troughs and folds appear well below the mean tropopause. Based on
 166 this map, the enhanced tropospheric O_3 finds its way into the stratosphere through isentropic
 167 flow across the jet streams into the extratropical lowermost stratosphere and also partly through
 168 ascent across the tropical tropopause. The stratospheric increases are asymmetric favoring the
 169 northern hemisphere because the tropospheric O_3 changes (O_3 minus O_3S) in the full chemistry
 170 model are driven by predominantly northern hemisphere emissions of ozone precursors. For our
 171 full chemistry run, the northern hemisphere (NH) and southern hemisphere (SH) trpcol O_3 are
 172 35.2 and 28.7 DU, respectively. For O_3S (30 ppb LBC), these values are 21.2 and 20.6 DU.
 173 Thus, the increase in trpcol O_3 is about twice as large in the NH as evidenced in Fig. 3. The small
 174 NH-SH difference in tropospheric O_3S reflects the nearly balanced STE O_3 flux in the UCI CTM
 175 (Ruiz and Prather, 2022), even though the SH flux has been reduced by about 14% due to the
 176 Antarctic ozone hole.



177
 178 Given our ability to measure trpcolO₃ from satellites (e.g. Ziemke et al., 2012) and the ready
 179 diagnostic of trpcolO₃ from the model intercomparison projects (MIPs: Young et al., 2013;
 180 Griffiths et al., 2021; Zeng et al., 2022), it would be great if we can derive a spillover factor that
 181 relates tropospheric column changes to the induced stratospheric column changes. For this
 182 study, we have available two independent cases: (i) the two Linoz runs with different LBCs, and
 183 (ii) the single modern full chemistry run that contrasts O₃ with O₃S. For these cases, the change
 184 in trpcolO₃ is an extremely poor predictor of strcolO₃ : (i) spillover factor of 0.13 DU per DU
 185 (1.6/12.4), and (ii) 0.34 DU per DU (3.8/11.0). Searching for a better predictor and considering
 186 Fig. 3, we identified the O₃ abundance (mole fraction) in the upper tropical troposphere,
 187 specifically the two model levels from 88 to 123 hPa. The predictor now is consistent for the
 188 two cases, 0.083 DU per ppb, but it is difficult, if not impossible, to observe the troposphere-only
 189 mole fraction of O₃ between 88 and 123 hPa except with sondes. Likewise, such a diagnostic for
 190 the MIPs would not work.

191 **3 Analysis of Past and Future Ozone Changes**

192 How can we use our limited set of CTM simulations to estimate the magnitude of the spillover
 193 effect from pre-industrial (PI) to present day (PD)? The change in trpcolO₃ from 1900 to 2000
 194 based on multi-model assessments give values of about +9 DU (Gauss et al., 2006; Young et al.,
 195 2013; Griffiths et al., 2021; Zeng et al., 2022), consistent with observed trends over the past two
 196 decades (Gaudel et al., 2018; Tarasick et al., 2019). We do not have the resources for a full PI to
 197 PD CTM simulation here and, further, lack the necessary PI meteorological data to drive the

198 transport. We propose that our Linoz 30 ppb simulation is similar to PI because: (1) trpcolO_3 is
 199 11 DU less than our PD simulation with full chemistry; (2) tropospheric O_3S is remarkably
 200 north-south symmetric; and (3) in most models tropospheric pollution-driven changes in O_3 are
 201 largest in the upper troposphere (e.g., Fig. 8 of Young et al., 2013, converting mass to
 202 abundance). Thus, assuming that the PI to PD profile of tropospheric O_3 has changed as in our
 203 O_3S to O_3 simulation, we scale our spillover (3.8 DU) with trpcolO_3 (from 11 to 9 DU) and get
 204 3.1 DU. Thus, our best estimate of the increase in strcolO_3 from PI to PD due simply to the
 205 increase in tropospheric O_3 is 3 DU. It is difficult to provide a formal error analysis, but our
 206 estimate would be ± 1.5 DU, due primarily to abundance uncertainty in the upper tropical
 207 troposphere.

208 How important is 3 DU spillover into strcolO_3 ? The difficulty, but necessity, of separating
 209 trends in total column O_3 (totcolO_3) into pollution-driven tropospheric and halogen-driven
 210 stratospheric is discussed in Box 3-3 of WMO (2022), but a reconciliation was not made. A
 211 global mean loss of about 8.0 DU in totcolO_3 is observed between 1980 and 2020 with most
 212 occurring before 1995 (see Fig. 3-6 of WMO, 2022). The return to 1980 O_3 levels is the
 213 established measure of “recovery” (Prather and Watson, 1990). The observed trpcolO_3 trend
 214 gives an increase of 3.6 DU for these four decades, and thus the true loss in strcolO_3 since 1980
 215 is 11.6 DU. The tropospheric spillover based on the increase in trpcolO_3 means that this inferred
 216 halogen-driven loss is further underestimated by 0.5 to 1.2 DU (The upper and lower range is
 217 based on trpcolO_3 spillover factors ranging from 0.34 (full chemistry O_3 -minus- O_3S) to 0.13
 218 (Linoz 30 ppb-minus-10 ppb cases)).

219 It is useful to examine the MIP-based attribution study of Zeng et al. (2022), which presented
 220 PI-PD changes in strcolO_3 and trpcolO_3 . Here we use year 2000 as PD for reading numbers from
 221 their figures. The PI-PD total change in trpcolO_3 is about +9.0 DU (consistent with previous
 222 studies); it is comprised of +4.0 DU from CH_4 increases and +7.5 DU from increased emissions
 223 of other O_3 precursors (e.g., NO_x , CO) minus the decreases driven by halocarbons and N_2O . The
 224 total change in strcolO_3 is predominantly negative (-14.5 DU) but with some large positive
 225 changes from CH_4 (+6.5 DU) and the other O_3 precursors (+2.5 DU) that parallel the trpcolO_3
 226 changes. The large direct role of CH_4 in stratospheric chemistry is well known and expected.
 227 What is unclear from the Zeng et al. analysis is whether the +2.5 DU from non- CH_4 precursors is
 228 a direct O_3 spillover effect from the +7.5 DU in trpcolO_3 or if it results from increased
 229 stratospheric chemical production of O_3 from the tropospheric NO_x entering the stratosphere or
 230 direct stratospheric emissions of aviation NO_x as described by Schmeltekopf (1992).

231 For the future, the multi-model assessments project changes in trpcolO_3 over the 21st century
 232 that vary by scenario from -5.6 DU (RCP2.6) to +5.3 DU (RCP8.5) to +7.3 DU (SSP3-7.0)
 233 (Archibald et al., 2020). This wide range is due primarily to changes in the O_3 precursor
 234 emissions and secondarily to recovery of halogen-driven depletion combined with overall
 235 climate change (e.g., warmer wetter troposphere, colder stratosphere). The spillover effect on
 236 strcolO_3 with the large factor (0.34 DU per DU) then ranges from -1.9 to +2.4 DU; but because
 237 these future changes likely preserve the current O_3 profile shape and hence have a smaller factor
 238 (0.13), the spillover is likely much smaller, -0.7 to +0.9 DU. For perspective, the totcolO_3 loss
 239 from 1900 to 2000 attributed to ozone depleting substances is about 20 DU, and the loss from all
 240 emissions is 14 DU (Zeng et al., 2022). In terms of the observed totcolO_3 loss since 1980, we
 241 are looking for recovery of about 8 DU. Thus the scenario range of projected changes in
 242 trpcolO_3 is comparable to size of the recovery (-70% to +90%), and the spillover effect onto

243 strcolO₃ will still be an important fraction (~25%). With fully diagnosed models, we should be
244 able recognize and correct for this, but with observations, the spillover effect is hidden within the
245 recovery and cannot be readily diagnosed.

246 **4. Discussion**

247 The spillover effect will vary depending on what is driving tropospheric O₃ changes and how
248 that is manifest in the upper tropical troposphere. It is necessary for other models to quantify this
249 effect, and to examine a range of scenarios. In simulating the spillover effect with other models,
250 one should avoid the use of tagged tracers such as labeling tropospheric O₃ and watching its
251 buildup in the stratosphere. Such experiments give unreliable results because tropospheric O₃
252 molecules entering the stratosphere are not differentiable from stratospheric O₃ molecules.
253 There are chemical feedbacks on O₃ and its lifetime (in parallel with tropospheric CH₄), and thus
254 addition of O₃ changes the whole of stratospheric O₃ chemistry, a process that cannot be simply
255 simulated with a tagged tracer (see the problems with O₃S as a measure of stratospheric
256 influence in Prather and Zhu, 2024). It is important that other model studies are able to
257 differentiate between the transport of O₃ (e.g., 10–30 % spillover) and that of chemical
258 precursors (NO_x, CH₄), and thus warrant such diagnostics in future ozone assessments.

259 The reverse of this process is well known, i.e., strcolO₃ changes propagate into the
260 troposphere through STE fluxes and alter trpcolO₃. Recent results allow us to quantify this. The
261 Antarctic ozone hole is shown to reduce the southern hemisphere STE ozone flux by on average
262 30 Tg-O₃ y⁻¹ with interannual variations of ± 20 Tg-O₃ y⁻¹ (Ruiz and Prather, 2022). Using the
263 24-day perturbation lifetime for tropospheric O₃ from STE sources, Prather and Zhu (2024)
264 calculate that the total STE perturbation is only 8%, and hence the SH mean reduction in
265 trpcolO₃ from the current ozone hole is only 0.4 DU. These relatively large ozone fluxes have
266 much less impact in the troposphere because the photochemistry is much more reactive (shorter
267 lifetime) there than in the lower stratosphere.

268 Unfortunately, this spillover effect exacerbates the conflicts inherent in environmental
269 mitigation strategy. For example, the RCP2.6 scenario greatly improves air quality by reducing
270 tropospheric O₃, but this leads to reductions in stratospheric O₃. Even the integrated O₃
271 depletion metric envisaged by Pyle et al. (2022) needs to be calculated with a full chemistry-
272 transport model that includes spillover effects when emission scenarios include O₃ precursors.

273 **Acknowledgments**

274 I am indebted to three anonymous reviewers and the editor for suggesting major revisions that
275 greatly improved the manuscript. The author declares no conflicts of interest relevant to this
276 study.

277 **Open Research - Data Availability Statement**

278 The UCI CTM output data used in the study are archived as netcdf files along with the plotted
279 data in Prather (2024).

280 **References**

285 Archibald, A.T., J. L. Neu, Y. F. Elshorbany, O. R. Cooper, P. J. Young, H. Akiyoshi, R. A. Cox, M. Coyle, R. G.
 286 Derwent, M. Deushi, A. Finco, G. J. Frost, I. E. Galbally, G. Gerosa, C. Granier, P. T. Griffiths, R. Hossaini,
 287 L. Hu, P. Jöckel, B. Josse, M. Y. Lin, M. Mertens, O. Morgenstern, M. Naja, V. Naik, S. Oltmans, D. A.
 288 Plummer, L. E. Revell, A. Saiz-Lopez, P. Saxena, Y. M. Shin, I. Shahid, D. Shallcross, S. Tilmes, T. Trickl, T.
 289 J. Wallington, T. Wang, H. M. Worden, G. Zeng (2020) Tropospheric Ozone Assessment Report: A critical
 290 review of changes in the tropospheric ozone burden and budget from 1850 to 2100, *Elementa: Science of the*
 291 *Anthropocene* (2020) 8 (1): 034, doi: 10.1525/elementa.2020.034

292 Cariolle, D., A. Lasserre-Bigory, and J. F. Royer (1990), A general circulation model simulation of the springtime
 293 Antarctic ozone and its impact on mid-latitudes, *J. Geophys. Res.*, 95(D2), 1883– 1898.

294 CIAP (1974) Climatic Impact Assessment Program, The Effects of Stratospheric Pollution by Aircraft, by A. J.
 295 Grobecker, S. C. Coroniti & R. H. Cannon Jr., ‘Report of Findings: Executive Summary’ and ‘Final Report.’
 296 DOT-TST-75-50 121974, Office of the Secretary of Transportation, Washington, D.C. 20590, xxvii + 134 pp.
 297 + appendixes of 674 pp.

298 Collins, W.J., Jean-François Lamarque, Michael Schulz, Olivier Boucher, Veronika Eyring, Michaela I. Hegglin,
 299 Amanda Maycock, Gunnar Myhre, Michael Prather, Drew Shindell, and Steven J. Smith (2016),
 300 AerChemMIP: Quantifying the effects of chemistry and aerosols in CMIP6, *Geosci. Model Dev.*, 10, 585–607,
 301 doi:10.5194/gmd-10-585-2017

302 Dubé, K., Randel, W., Bourassa, A., & Degenstein, D. (2022). Tropopause-level NO_x in the Asian summer
 303 monsoon. *Geophysical Research Letters*, 49, e2022GL099848. doi: 10.1029/2022GL099848

304 Fu, R., Hu, Y., Wright, J.S., Jiang, J.H., Dickinson, R.E., Chen, M., Filipiak, M., Read, W.G., Waters, J.W., Wu,
 305 D.L. (2006) Short circuit of water vapor and polluted air to the global stratosphere by convective transport over
 306 the Tibetan Plateau. *Proc Natl Acad Sci U S A*. 103(15): 5664-5669. doi: 10.1073/pnas.0601584103

307 Gaudel, A., O.R. Cooper, G. Ancellet, B. Barret, A. Boynard, J.P. Burrows, C. Clerbaux, P.-F. Coheur, J. Cuesta, E.
 308 Cuevas, S. Doniki, G. Dufour, F. Ebojje, G. Foret, O. Garcia, M.J. Granados-Muñoz, J.W. Hannigan, F. Hase,
 309 B. Hassler, G. Huang, D. Hurtmans, D. Jaffe, N. Jones, P. Kalabokas, B. Kerridge, S. Kulawik, B. Latter, T.
 310 Leblanc, E. Le Flochmoën, W. Lin, J. Liu, X. Liu, E. Mahieu, A. McClure-Begley, J.L. Neu, M. Osman, M.
 311 Palm, H. Petetin, I. Petropavlovskikh, R. Querel, N. Rahpoe, A. Rozanov, M.G. Schultz, J. Schwab, R.
 312 Siddans, D. Smale, M. Steinbacher, H. Tanimoto, D.W. Tarasick, V. Thouret, A.M. Thompson, T. Trickl, E.
 313 Weatherhead, C. Wespes, H.M. Worden, C. Vigouroux, X. Xu, G. Zeng, & J. Ziemke (2018) Tropospheric
 314 Ozone Assessment Report: Present-day distribution and trends of tropospheric ozone relevant to climate and
 315 global atmospheric chemistry model evaluation, *Elementa: Science of the Anthropocene*, 6, 39, doi:
 316 10.1525/elementa.291.

317 Gauss, M., G. Myhre, I.S.A. Isaksen, W.J. Collins, F.J. Dentener, K. Ellingsen, L.K. Gohar, V. Grewe, D.A.
 318 Hauglustaine, D. Iachetti, J.-F. Lamarque, E. Mancini, L.J. Mickley, G.Pitari, M.J. Prather, J.A. Pyle, M.G.
 319 Sanderson, K.P. Shine, D.S. Stevenson, K. Sudo, S. Szopa, O. Wild, G. Zeng (2006), Radiative forcing since
 320 preindustrial times due to ozone change in the troposphere and the lower stratosphere, *Atmos. Chem. Phys.*, 6,
 321 575–599, doi: 10.5194/acp-6-575-2006

322 Gettelman, A., and S. L. Baugheum (1999), Direct deposition of subsonic aircraft emissions into the stratosphere, *J.
 323 Geophys. Res.*, 104(D7), 8317–8327, doi:10.1029/1999JD900070.

324 Griffiths, P. T., Murray, L. T., Zeng, G., Shin, Y. M., Abraham, N. L., Archibald, A. T., Deushi, M., Emmons, L. K.,
 325 Galbally, I. E., Hassler, B., Horowitz, L. W., Keeble, J., Liu, J., Moeini, O., Naik, V., O'Connor, F. M.,
 326 Oshima, N., Tarasick, D., Tilmes, S., Turnock, S. T., Wild, O., Young, P. J., & Zanis, P. (2021) Tropospheric
 327 ozone in CMIP6 simulations, *Atmos Chem Phys*, 21, 4187-4218, 10.5194/acp-21-4187-2021.

328 Hirsch, E., and I. Koren (2021) Record-breaking aerosol levels explained by smoke injection into the stratosphere.
 329 *Science* 371, 1269-1274. doi: 10.1126/science.abe1415

330 Hsu, J., and M. J. Prather (2009), Stratospheric variability and tropospheric ozone, *J. Geophys. Res.*, 114, D06102.
 331 doi:10.1029/2008JD010942

332 Hsu, Juno & M. J. Prather (2010), Global long-lived chemical modes excited in a 3-D chemistry transport model:
 333 Stratospheric N₂O, NO_y, O₃ and CH₄ chemistry, *Geophys. Res. Lett.*, 37, L07805, doi:
 334 10.1029/2009GL042243.

335 Hsu, Juno and M. J. Prather (2010), Global long-lived chemical modes excited in a 3-D chemistry transport model:
 336 Stratospheric N₂O, NO_y, O₃ and CH₄ chemistry, *Geophys. Res. Lett.*, 37, L07805,
 337 doi:10.1029/2009GL042243.

338 Johnston, H.S. (1971) Reduction of stratospheric ozone by nitrogen oxide catalysts from supersonic transport
 339 exhaust. *Science*, 173, pp. 517-22, DOI: 10.1126/science.173.3996.517

340 Lelieveld, J., E. Bourtsoukidis, C. Brühl, H. Fischer, H. Fuchs, H. Harder, A. Hofzumahaus, F. Holland, D. Marno,
 341 M. Neumaier, A. Pozzer, H. Schlager, J. Williams, A. Zahn, H. Ziereis (2018) The South Asian monsoon –
 342 pollution pump and purifier. *Science*, 361: 270-273. doi: 10.1126/science.aar2501

343 McElroy, M.B., Wofsy, S.C., Penner, J.E. & McConnell, J. C. (1974) Atmospheric ozone: possible impact of
 344 stratospheric aviation. *Journal of Atmospheric Sciences*, 31, pp. 287-300, doi: 10.1175/1520-
 345 0469(1974)031<0287:AOPIOS>2.0.CO;2.

346 McLinden, C., S. Olsen, B. Hannegan, O. Wild, M. Prather, and J. Sundet (2000) Stratospheric ozone in 3-D
 347 models: a simple chemistry and the cross-tropopause flux, *J. Geophys. Res.*, 105, 14653-14665.

348 Molina, M.J. and F.S. Rowland (1974) Stratospheric sink for chlorofluoromethanes: chlorine atom-catalysed
 349 destruction of ozone, *Nature* 249, 810–812, doi:10.1038/249810a0

350 Oman, L.D., A.R. Douglass, R.J. Salawitch, T.P. Carty, J.R. Ziemke, and M. Manyin (2016), The effect of
 351 representing bromine from VSLS on the simulation and evolution of Antarctic ozone, *Geophys. Res.*
 352 Lett., 43,9869–9876, doi:10.1002/2016GL070471

353 Prather, M.J. (2024), UCI CTM model simulations used for deriving the spillover of tropospheric ozone into the
 354 stratosphere, [Dataset]. Dryad. <https://doi.org/10.5061/dryad.dr7sqvb66>

355 Prather, M.J. and R.T. Watson (1990) Stratospheric ozone depletion and future levels of atmospheric chlorine and
 356 bromine, *Nature*, 334, 729-734.

357 Prather, M.J. and Xin Zhu (2024) Lifetimes and timescales of tropospheric ozone, *Elementa: Science of the*
 358 *Anthropocene*, 12 (1): 00112, doi: 10.1525/elementa.2023.00112

359 Prather, M.J., X. Zhu, Q. Tang, J. Hsu, & J.L. Neu (2011), An atmospheric chemist in search of the tropopause, *J.*
 360 *Geophys. Res.*, 116: D04306, doi:10.1029/2010JD014939.

361 Pyle, J.A., Keeble, J., Abraham, N.L., Chipperfield, M.P. & Griffiths, P.T. (2022), Integrated ozone depletion as a
 362 metric for ozone recovery. *Nature* 608, 719–723. doi: 10.1038/s41586-022-04968-8

363 Randel, W.J., M. Park, L. Emmons, D. Kinnison, P. Bernath, K.A. Walker, C. Boone, H. Pumphrey (2010) Asian
 364 monsoon transport of pollution to the stratosphere. *Science* 328(5978):611-3. doi: 10.1126/science.1182274.

365 Reader, M. C., D. A. Plummer, J. F. Scinocca, and T. G. Shepherd (2013), Contributions to twentieth century total
 366 column ozone change from halocarbons, tropospheric ozone precursors, and climate change, *Geophys. Res.*
 367 Lett., 40, 6276–6281, doi:10.1002/2013GL057776.

368 Ruiz, D. J. & M.J. Prather (2022) From the middle stratosphere to the surface, using nitrous oxide to constrain the
 369 stratosphere–troposphere exchange of ozone, *Atmos. Chem. Phys.*, 22, 2079–2093, doi: 10.5194/acp-22-2079-
 370 2022.

371 Santee, M. L., Lambert, A., Manney, G. L., Livesey, N. J., Froidevaux, L., Neu, J. L., et al. (2022). Prolonged and
 372 pervasive perturbations in the composition of the Southern Hemisphere midlatitude lower stratosphere from the
 373 Australian New Year's fires. *Geophysical Research Letters*, 49, e2021GL096270. doi: 10.1029/2021GL096270

374 Schmeltekopf, A.L. (1992) *Chapter 6: Lower Stratospheric Measurement Issues in The High-Speed Research*
 375 *Program / Atmospheric Effects of Stratospheric Aircraft, A First Program Report* (eds., M.J. Prather and H.L.
 376 Wesoky), NASA Reference Publication 1272, Jan 1992, 244 pp.,
 377 <https://ntrs.nasa.gov/api/citations/19920009879/downloads/19920009879.pdf>

378 Shindell, D., Faluvegi, G., Nazarenko, L., Bowman, K., Lamarque, J. F., Voulgarakis, A., ... Ruedy, R. (2013).
 379 Attribution of historical ozone forcing to anthropogenic emissions. *Nature Climate Change*, 3(6), 567–570. doi:
 380 10.1038/nclimate1835

381 Solomon, S., K. Dubeb, K. Stonea, and 13 others (2022) On the stratospheric chemistry of midlatitude wildfire
 382 smoke, *PNAS* 119(10), e2117325119, doi: 10.1073/pnas.2117325119

383 Stolarski, R.S. and R. J. Cicerone. 1974. Stratospheric Chlorine: a Possible Sink for Ozone. *Canadian Journal of*
 384 *Chemistry*. 52(8): 1610-1615. <https://doi.org/10.1139/v74-233>

385 Tarasick, David, Ian E. Galbally, Owen R. Cooper, Martin G. Schultz, Gerard Ancellet, Thierry Leblanc, Timothy J.
 386 Wallington, Jerry Ziemke, Xiong Liu, Martin Steinbacher, Johannes Staehelin, Corinne Vigouroux, James W.
 387 Hannigan, Omaira García, Gilles Foret, Prodromos Zanis, Elizabeth Weatherhead, Irina Petropavlovskikh,
 388 Helen Worden, Mohammed Osman, Jane Liu, Kai-Lan Chang, Audrey Gaudel, Meiyun Lin, Maria Granados-
 389 Muñoz, Anne M. Thompson, Samuel J. Oltmans, Juan Cuesta, Gaelle Dufour, Valerie Thouret, Birgit Hassler,
 390 Thomas Trickl, Jessica L. Neu (2019) Tropospheric Ozone Assessment Report: Tropospheric ozone from 1877
 391 to 2016, observed levels, trends and uncertainties. *Elementa: Science of the Anthropocene* 1 January 2019; 7
 392 39. doi: <https://doi.org/10.1525/elementa.376>

393 Wales, P.A., Salawitch, R.J., Nicely, J.M. et al. (46 more authors) (2018) Stratospheric Injection of Brominated
 394 Very Short-Lived Substances: Aircraft Observations in the Western Pacific and Representation in Global

395 Models. *Journal of Geophysical Research: Atmospheres*, 123 (10). pp. 5690-5719. doi:
 396 10.1029/2017JD027978

397 Wild, O. and M.J. Prather (2000) Excitation of the primary tropospheric chemical mode in a global three-
 398 dimensional model, *J. Geophys. Res.*, 105, 24647-24660.

399 Wild, O., J.K. Sundet, M.J. Prather, I.S.A. Isaksen, H. Akimoto, E.V. Browell, and S.J. Oltmans (2003) CTM Ozone
 400 Simulations for Spring 2001 over the Western Pacific: Comparisons with TRACE-P lidar, ozonesondes and
 401 TOMS columns, *J. Geophys. Res.*, 108(D21), 8826, doi:10.1029/2002JD003283.

402 WMO (1981) The Stratosphere 1981: Theory and Measurements. WMO Global Ozone Research and Monitoring
 403 Project Report No. 11, World Meteorological Organization, Geneva, Switzerland

404 WMO (1985) Atmospheric Ozone 1985: Assessment of Our Understanding of the Processes Controlling Its Present
 405 Distribution and Change, World Meteorological Organization, Global Ozone Research And Monitoring
 406 Project, Report No. 16, 3 Vol, 1095 pp + 86 pp, <https://csl.noaa.gov/assessments/ozone/1985/report.html>
 407 (accessed 21 Mar 2024).

408 WMO (2022) World Meteorological Organization. Executive Summary. Scientific Assessment of Ozone Depletion:
 409 2022, GAW Report No. 278, 56 pp.; WMO: Geneva, Switzerland.
 410 <https://csl.noaa.gov/assessments/ozone/2022/downloads/> (accessed 21 Mar 2024)

411 Wofsy, S.C., and M. B. McElroy (1974) HO_x, NO_x and C₁O_x: Their role in atmospheric photochemistry, *Can. J.
 412 Chem.*, 52, 1582-1591, DOI: 10.1139/v74-230

413 Young, P. J., Archibald, A. T., Bowman, K. W., Lamarque, J.-F., Naik, V., Stevenson, D. S., Tilmes, S.,
 414 Voulgarakis, A., Wild, O., Bergmann, D., Cameron-Smith, P., Cionni, I., Collins, W. J., Dalsøren, S. B.,
 415 Doherty, R. M., Eyring, V., Faluvegi, G., Horowitz, L. W., Josse, B., Lee, Y. H., MacKenzie, I. A.,
 416 Nagashima, T., Plummer, D. A., Righi, M., Rumbold, S. T., Skeie, R. B., Shindell, D. T., Strode, S. A., Sudo,
 417 K., Szopa, S., & Zeng, G. (2013) Pre-industrial to end 21st century projections of tropospheric ozone from the
 418 Atmospheric Chemistry and Climate Model Intercomparison Project (ACCMIP), *Atmos. Chem. Phys.*, 13,
 419 2063–2090, <https://doi.org/10.5194/acp-13-2063-2013>.

420 Young, P. J., Naik, V., Fiore, A. M., Gaudel, A., Guo, J., Lin, M. Y., Neu, J. L., Parrish, D. D., Rieder, H. E.,
 421 Schnell, J. L., Tilmes, S., Wild, O., Zhang, L., Ziemke, J., Brandt, J., Delcloo, A., Doherty, R. M., Geels, C.,
 422 Hegglin, M. I., Hu, L., Im, U., Kumar, R., Luhar, A., Murray, L., Plummer, D., Rodriguez, J., Saiz-Lopez, A.,
 423 Schultz, M. G., Woodhouse, M. T., & Zeng, G., (2018) Tropospheric Ozone Assessment Report: Assessment
 424 of global-scale model performance for global and regional ozone distributions, variability, and trends,
 425 *Elementa: Science of the Anthropocene*, 1 January 2018; 6 10. doi: /10.1525/elementa.265

426 Zeng, G., Morgenstern, O., Williams, J.H. T., O'Connor, F. M., Griffiths, P. T., Keeble, J., et al. (2022). Attribution
 427 of stratospheric and tropospheric ozone changes between 1850 and 2014 in CMIP6 models. *Journal of
 428 Geophysical Research: Atmospheres*, 127, e2022JD036452. <https://doi.org/10.1029/2022JD036452>.

429 Ziemke, J. R. & Chandra, S. (2012) Development of a climate record of tropospheric and stratospheric column
 430 ozone from satellite remote sensing: evidence of an early recovery of global stratospheric ozone, *Atmos.
 431 Chem. Phys.*, 12, 5737–5753, <https://doi.org/10.5194/acp-12-5737-2012>